NUMERICAL STUDY OF SUPERCRITICAL WATER HEAT TRANSFER IN VERTICAL BARE TUBES USING FLUENT CFD CODE

Amjad Farah, Maxim Kinakin, Igor Shevchuk*, Glenn Harvel and Igor Pioro

Faculty of Energy Systems and Nuclear Science
University of Ontario Institute of Technology
2000 Simcoe Str. N., Oshawa ON L1H 7K4 Canada

** MBtech Group GmbH & Co. KGaA, Salierstr. 38, 70736 Fellbach-Schmiden, Germany*

Abstract

In this paper, a numerical study of heat transfer in supercritical water flowing upwards in vertical bare tubes using the Computational Fluid Dynamics (CFD) code FLUENT-12 is presented. A large dataset was collected for conditions similar to those of SuperCritical Water-cooled Reactors (SCWRs) at the Institute for Physics and Power Engineering at Obninsk, Russia. This set includes 80 runs in a 4-m long, 10-mm inside diameter vertical bare tube within a wide range of operating parameters: pressure of 24 MPa, inlet temperatures from 320 to 350°C, values of mass flux ranged from 200 – 1500 kg/(m^{2}s) and heat fluxes up to 1250 kW/m^2, for several combinations of wall and bulk-fluid temperatures, which were below, at, or above the pseudocritical temperature (381^{o}C at 24 MPa).

Complete analysis of the SCW properties in the tube was done using an axisymmetric 2D-model of the tube with 10,000 nodes along the length of the tube for optimal results. Two viscous models were used in the process: 1) k-ε model with enhanced wall treatment and pressure gradient and thermal effects, and 2) k-ω SST model with low Re corrections and viscous heating. Results show a good fit for most low/mid range operating conditions with noticeable deviations at high range primarily in the deteriorated heat-transfer regime, with overall better fit for k-ε model.

FLUENT showed a better fit for experimental results for the low heat and mass fluxes than empirical correlations, but FLUENT still shares the same problem in predicting the deteriorated heat-transfer regime accurately. FLUENT also shows some deviation from the experimental data within the entrance region for high heat and mass fluxes, associated with the level of flow development in the tube which is attributable to entrance turbulence modelling.

1. Introduction

Gen-IV reactors are currently being designed worldwide, and Canada has adopted an SCWR concept in which SCW is considered as a coolant. Experiments and heat transfer correlations are in the early stages of capturing the various phenomena expected to occur in such designs [1].

Currently, there is only one supercritical-water heat-transfer correlation for use in fuel bundle geometries. This correlation was obtained for a helically finned 7-element bundle and was developed by Dyadyakin and Popov [2].

In addition, the main problem with the correlations and models developed to date is that only 1D affects have been captured. Performing experiments that will accurately capture 3-D effects are very expensive; hence an alternative approach is needed. CFD research has been performed in this area in attempts to determine 3-D effects of heat and mass transfer within the fuel subchannels [3]. Most modeling experts in the nuclear industry support the approach of using CFD codes such as FLUENT to analyze 3-D effects [4, 5, and 6]. However the accuracy of CFD codes for SCW is not well known at this time [7]. A study of well known experimental datasets is needed to verify their accuracy against empirical correlations used for the same purpose.

Canada's contribution to the fourth generation of nuclear power reactor designs entails a CANDU type design utilizing horizontal pressure tubes and heavy water as moderator. The main difference between Gen-III CANDUs and the new Gen-IV design is the use of SCW as a coolant. Use of a supercritical fluid allows for higher pressures and outlet temperatures, and thus an increase in overall plant efficiencies from the current 30-35% to 45-50% [8]. Design of the CANDU Gen-IV SCWR requires knowledge of the thermalhydraulic conditions existing within the pressure tubes. To determine these conditions, an advanced toolset including CFD codes is necessary. The CFD code must be rigorously tested before it may be deemed accurate enough to be applied to SCWR simulations. CFD codes are routinely used in the nuclear industry in attempts to quantify flow effects under normal operating and accident type scenarios [3], but none have been validated for use under supercritical conditions. In this work, assessment of the capability of the CFD code FLUENT-12 to capture heat transfer phenomenon of SCW flowing through a vertical bare tube is performed with the specific objective to determine limitations and capabilities near the pseudocritical point.

2. Methodology

A dataset provided by Kirillov et al. from the Institute for Physics and Power Engineering (Obninsk, Russia) was used for this study [8]. The dataset was previously analyzed using many empirical correlations, where the Mokry et al. correlation showed to have the best fit under the given operating parameters [9]. Hence the Mokry et al. correlation was chosen for comparison with the CFD FLUENT-12 results. The Mokry et al. correlation used in the comparison is shown below:

$$\mathbf{Nu_b} = 0.0061\, \mathbf{Re_b^{0.904}}\, \overline{\mathbf{Pr}}_{\mathbf{b}}^{\mathbf{0.684}} \left(\frac{\rho_w}{\rho_b}\right)^{0.564} \tag{1}$$

However, since this correlation was meant for use only at normal heat transfer (NHT) and improved heat transfer (IHT) regimes, an empirical correlation shown in equation 2 was proposed for deteriorated heat-flux calculations in which the DHT appears (for details, see reference [10]):

$$q_{dht} = -58.97 + 0.745\, G, \text{ kW/m}^2 \tag{2}$$

Kirillov's experiments with SCW provide data which can be used to benchmark the ability of the FLUENT code in solving heat and mass transfer problems in the supercritical region. The Kirillov experiments consist of a four-meter long vertically oriented pipe of inner and outer diameter of 10mm and 14mm respectively. The pipe was constructed of steel, with an average surface roughness height of 0.7 μm. Table 1 identifies the range of conditions for the Kirillov experiments, and the highlighted region represents similar operating parameters ranges to the ones expected in normal operating conditions of SCWRs of interest to Canada.

Table 1: Kirillov Data Ranges of SCW Experimental Data [8]

Mass Flux (kg/m^2s)	**Pressure range (MPa)**	**Bulk Fluid Temperature (°C)**	**Heat Flux Range (kW/m^2)**
200	24.0 – 24.1	320 – 450	73 – 214
500	24.0 – 24.1	325 – 450	141 – 454
1,000	23.9 – 24.1	325 – 425	392 – 826
1,500	24.0 – 24.1	320 – 425	489 – 1,256

Subcritical water was pumped upwards through the test section at four different mass fluxes of 200, 500, 1,000, and 1,500$\frac{kg}{m^2 s}$. Each group of mass flux was pumped through the test section and heated by passing an electrical current through the pipe. The effective surface heat flux was varied between the range 73−1,256 $\frac{kW}{m^2}$. All runs had an inlet pressure of 24±0.1 MPa. For each group of mass flux, the inlet temperature was varied so that the enthalpy increase along the length of the pipe varies within the group. The inlet temperature was set to less than 25°C from the pseudocritical point in each case to capture subtle changes approaching the pseudocritical point. Some of the low heat flux cases were modeled so that the pseudocritical point is located just before the fluid exits the heated length. Table 2 shows the uncertainties in measuring the various abovementioned parameters.

Table 2: Uncertainties in Primary Parameters [8]

Parameter	**Maximum Uncertainty**
Test-section power	±1.0%
Inlet pressure	±0.25%
Wall temperature	±3.0%
Mass-flow rate	±1.5%
Heat loss	≤3.0%

2.1 Initial graphical model and mesh

Initially, a 3-D model was constructed using the Gambit software (geometry modeler and numerical grid generator), which was then exported to FLUENT-12 CFD code for CFD analysis. The 3-D model included various mesh sizes of 4,000, 8,000 and 10,000 nodes along the length of the tube, with 120 and 240 nodes in the radial direction. In addition, a boundary layer was introduced to account for the viscous effects near the inside wall. After testing of the different combinations of meshes, the best results (in terms of convergence and accuracy in predicting experimental results) were obtained from the 10,000 axial and 240 radial divisions, with a boundary layer thickness of 21 microns. The mesh, however successful, proved to be very consuming in both time and computation power in each simulation. The study diverted in the direction of a 2-D axisymmetric model, as a base to select the best viscous model comparable to 3-D models but would save valuable computation time and resources.

A mesh independence study was carried out to determine the validity of the FLUENT output. Mesh independence is reached once any further refinement of a given mesh does not produce significant changes in the computed solution. It is essential that this test be carried out to ensure that the most accurate result is obtained from a given CFD model.

Table 3 shows the evolution of the mesh and the computer memory consumption. The FLUENT-12 and Gambit software were 32-bit versions, and as such they were limited to a maximum of 3GB of RAM. Attempts were made to test finer meshes, but the available resources did not allow this continuation.

Table 3: Differences in Mesh Sizes

Mesh Name	Axial Divisions	Radial Divisions	Element Count	Memory Usage
Original	8,000	100	8×10^5	~1.3 GB
Coarse	4,000	80	3.2×10^5	~800 MB
Fine	10,000	120	1.2×10^6	~2 GB

2.2 Material selection and SCW properties

The tube inner surface material was selected to be steel just as in the Kirillov experiment. The steel properties were provided by the FLUENT-12 database of materials. However, the SCW is not included in this database, and the properties of SCW had to be introduced to FLUENT-12 by other means. Three methods were explored in this aspect:

1) Using MATLAB to create equations that best represent the SCW properties, including density, viscosity, thermal conductivity and specific heat. This method was proved to be flawed because FLUENT-12 only accepts polynomial functions and only for 3 range of temperature for each property. This meant sacrificing accuracy, in order to cover the range of each property, because the thermophysical properties of water change dramatically around the pseudocritical point (±25°C) as shown in Figure 1.
2) The second method is using User Defined Functions (UDFs), which are written using the programming language C++. UDFs include headers and C++ files that are then compiled in FLUENT-12 producing the functions to describe any property of the SCW. This approach provides more flexibility in defining the type of function (not limited to polynomials), and the temperature ranges (not limited to 3). The problems in this method however, arose in compiling the UDFs in FLUENT-12. Increasing the number of temperature ranges, and the complexity of the functions, caused a strain on the computational ability of the computers, and multiple software crashes while compiling the functions. This is in addition to the fact that only a constant pressure is assumed (24 MPa) for the properties, which is not accurate for the whole dataset.

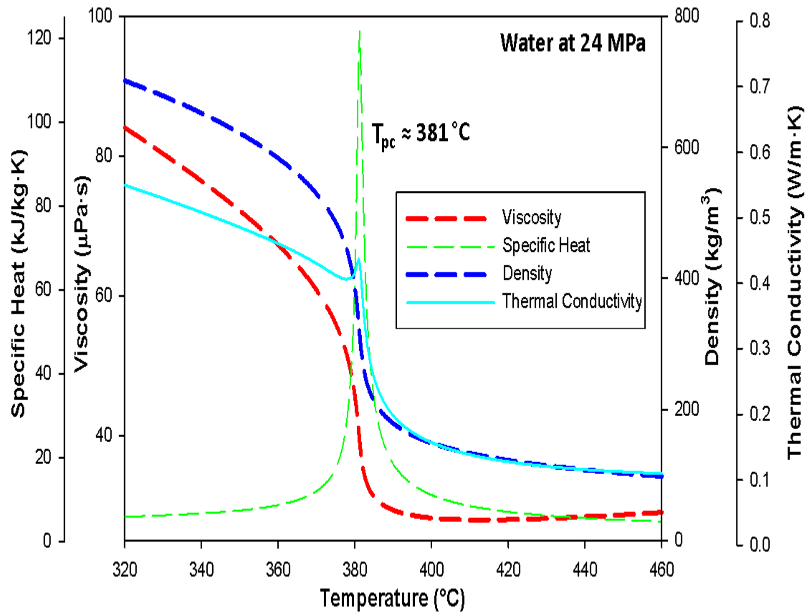

Figure 1: Thermophysical Properties of Water at 24 MPa.

3) The third and selected method was to establish an interface between FLUENT-12 and NIST REFPROP 8.0 [11] by the means of command lines written in the command window of FLUENT-12.

2.3 CFD theory and viscous model selection

The most well known two-equation energy transport turbulence model is the *k-ε* turbulence model developed by Jones & Launder [12]. The variables k and ϵ represent the total turbulent kinetic energy and the dissipation rate of said energy respectively. These variables account for the amount of kinetic energy present within an eddy, and the rate at which that energy is dissipated to the flowing fluid. The model works by conserving the energy contained within a turbulent region through transport equations that carry that total energy (and its dissipation) along a geometrical flow path. The two quantities are described as follows:

$$k = \frac{u^2+v^2+z^2}{2} \qquad \left(\frac{m^2}{s^2}\right) \tag{3}$$

Where u, v, and z represent the one dimensional velocities of the fluid. The variable ε is dependent on k as well as the eddy viscosity, which governs the transport of kinetic turbulent energy, and is analogous to the how molecular viscosity governs the transport of momentum of in a flowing fluid. The dissipative energy term ϵ is described as follows:

$$\epsilon = \rho C_\mu \frac{k^2}{\mu_t} \qquad \left(\frac{m^2}{s^3}\right) \tag{4}$$

Where ρ is the density of the fluid, μ_t is the eddy viscosity, and C_μ is a constant taken to be 0.09 as defined by the standard *k-ε* model.

Another model was developed to improve the accuracy of *k-ε* model due to its dependence on a single turbulent length scale, and Wilcox developed the *k-ω* model [13] that removes this dependence, allowing for solutions encompassing any size of turbulent eddy generation. ω represents the specific turbulent energy dissipation rate, and defined in terms of k and ε as follows:

$$\omega = \frac{\epsilon}{k} \qquad (s^{-1}) \tag{5}$$

However, this model was very sensitive to free stream values of ω far from the boundary layer, which called for the development of the *k-ω* Shear Stress Transport (SST) to overcome this deficiency [14].

Each of these models incorporates many options such as enhanced wall treatment, thermal effects, viscous heating, low-Re corrections, etc. And the selection of the best model meant running multiple simulations in each of them to discover the various phenomena predicted by each. All simulations were performed using a coupled pressure-velocity solver, and the solutions to transport equations were conducted using second order algorithms. Analysis was performed with the Realizable *k-ε* model with enhanced wall treatment, pressure gradient effects, thermal effects, viscous heating and full buoyancy effects and *k-ω* SST with low-Re corrections and viscous heating.

2.4 Entrance region effect

Initial simulations showed that small discontinuities resulted near the inlet of the domain with significant over-prediction of the wall temperature. The likely contribution to the over-prediction was modeling the flow as a uniform velocity at the inlet. An entrance region consists of 20cm (20 pipe diameters) was added to the inlet to allow for the fluid flow to naturally develop before entering the heated length. This entrance region was meshed such that its divisions had the same spacing as that of the heated length to ensure continuity of the results. The extra unheated length of mesh had to be declared as an interface zone within FLUENT, removing the discontinuity between the two meshes. While this addition to the mesh reduced the size of the discontinuities near the inlet, the entrance region was not always able to fully remove the discontinuities. The entrance region did however appear to reduce discontinuities for the lower mass flux regimes, but the discontinuities still persist in the high mass flux range. This is particularly unfortunate as applying these turbulence models to SCWR design will surely require even higher mass fluxes than those tested by Kirillov et al. It is certainly possible to continue to extend this entrance region, however in doing so the geometric model inevitably distances itself from the physical test matrix used in the experiments. The final mesh used in the simulations is shown in figure 2.

To give an example of how the results varied before and after the addition of the entrance region, Figure 3 (a) displays how all tested models experience the entrance effect, while 3 (b) shows how *k-ε* (shown in green in both figures) changes profile and shows the absence of fluctuations. In the case where no entrance region is used, there are perturbations in the wall temperature at 0.5 and 1.1 m, which cause significant perturbations in the heat transfer coefficients. This has a downstream effect on all of the prediction. When an entrance region is used to develop the flow, the perturbations disappear. Hence, entrance effects are critical to modeling the experiment.

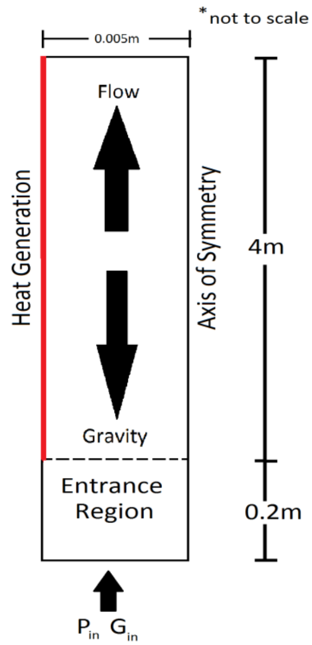

Figure 2: Graphical representation of computation domain

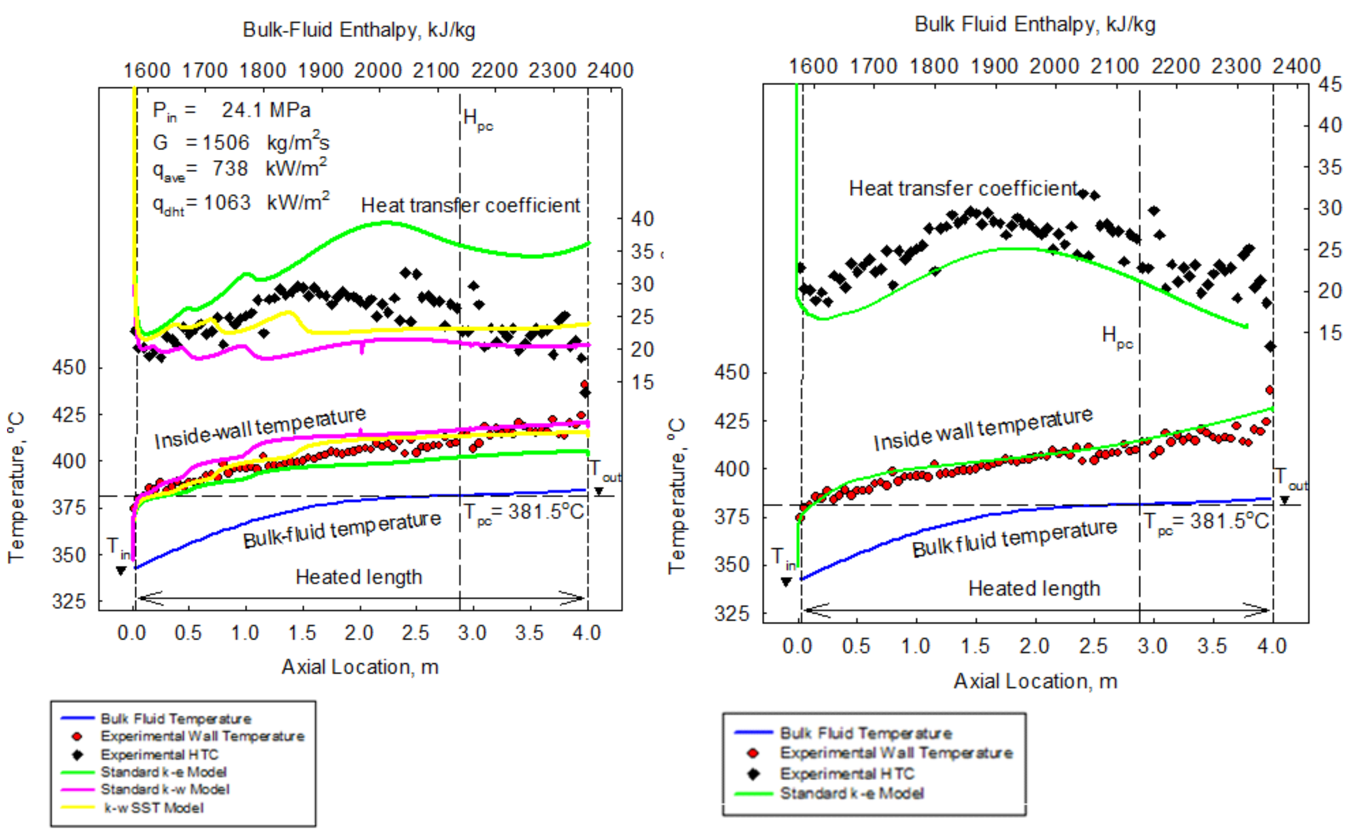

(a) No entrance region (b) With entrance region

Figure 3: Effects of adding an entrance region to the mesh.

3. Numerical results and analysis

As interest lays mainly in conditions similar to the operating parameter of SCWR's, the results shown here are for comparatively high mass fluxes of 1,000-1,500 kg/(m^{2}s). Figure 4 shows the results of a mid-range mass flux with low heat flux parameters. Residing in the normal heat transfer regime (NHT) with the pseudocritical point existing at the end of the tube, both models gave satisfactory results for prediction of bulk-fluid temperature, wall temperature and heat transfer coefficients. Both models resulted in a more conservative approach than the Mokry et al. correlation as shown in Figure 4.

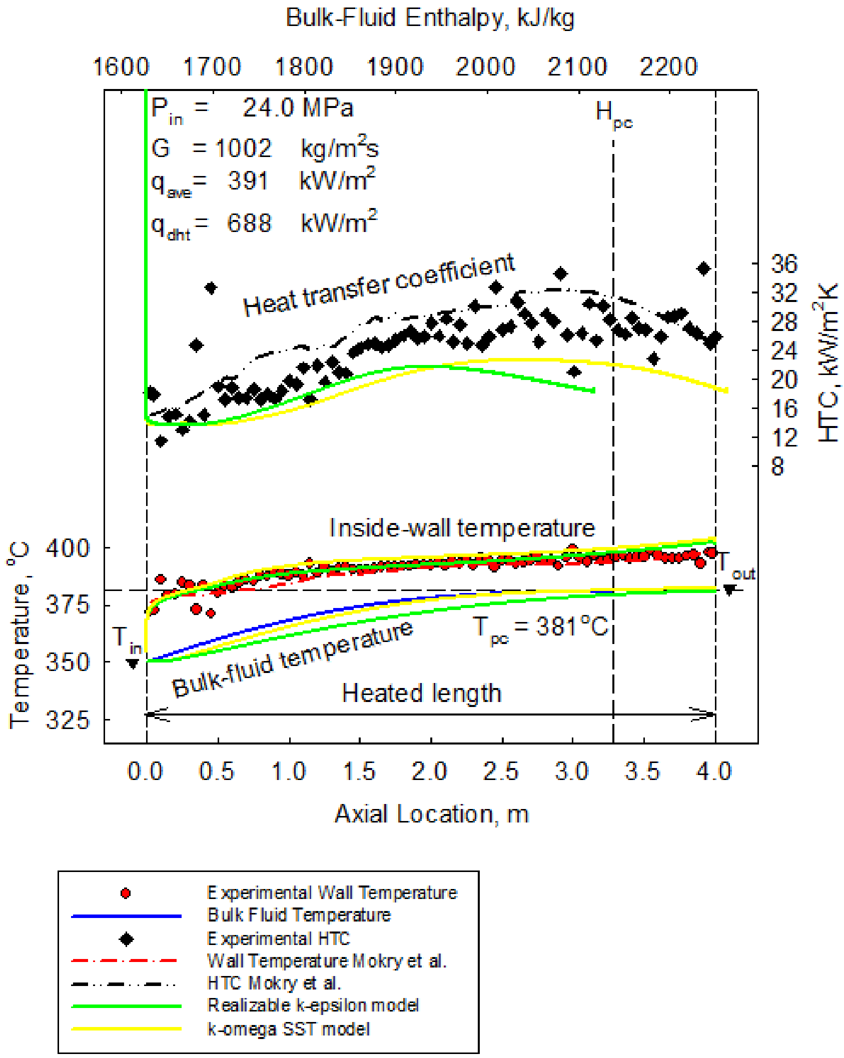

Figure 4: Experimental, calculated, and simulated results for mid-range mass flux (1002 kg/(m^{2}s)), and low-range heat flux, below DHT regime (391 kW/m^2).

Figure 5 shows a case where deteriorated heat transfer regime and the pseudocritical region both have significant impacts on the results of the simulation. Near the pseudocritical point, the RKE model deviates from the experimental results and shows an overestimation of wall temperatures. At an earlier axial position, SST *k-ω* suffers further by introducing a discontinuity of almost 200 degrees for the computed wall temperature, but stabilizes after about one meter of heated length. While good agreement exists before the pseudocritical point, it is apparent that future investigation with the predictive capability of FLUENT is necessary.

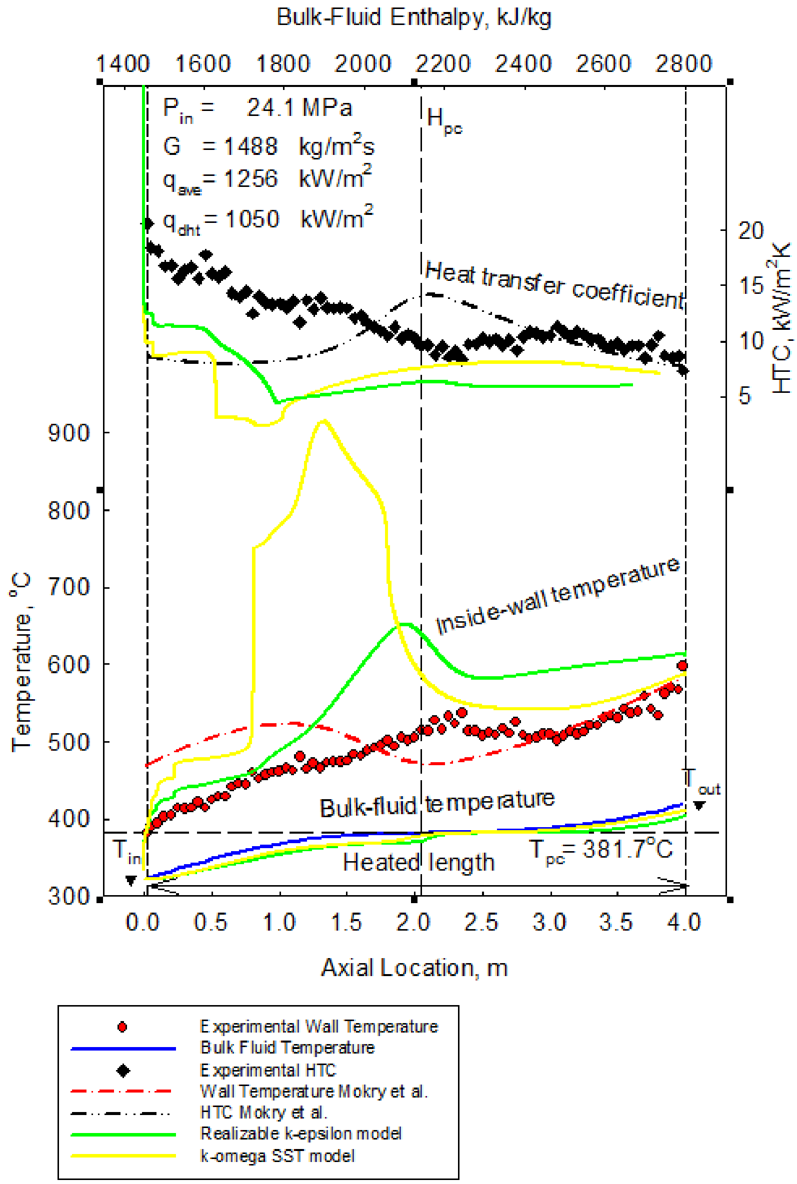

Figure 5: Experimental, calculated, and simulated results for DHT case with high mass flux (1488 kg/(m^{2}s)) and high heat flux (1256 kW/m^2).

Error! Reference source not found.Error! Reference source not found. and **Error! Reference source not found.** show the difference between the experimental and simulated values for enthalpy change, bulk fluid temperature change, and average HTC values for a number of simulations, in both RKE and *k-ω* SST to show the general behavior of FLUENT-12 over multiple runs. The ranges for the figures are mass fluxes of 500-1500 kg/(m^{2}s), and heat fluxes of 236-1094 kW/m^2. The total enthalpy rise along the heated length are all enclosed in the ±10% uncertainty. The average bulk fluid change uncertainty is also relatively small, mainly between 0 and -10% which means an underprediction on the side of FLUENT-12 using both turbulence models. Finally, the average HTC values we compared, and for both turbulence models, it shows underprediction of up to -30% from the experimental values, which is still around the same uncertainty as the Mokry et al. correlation for HTC calculations.

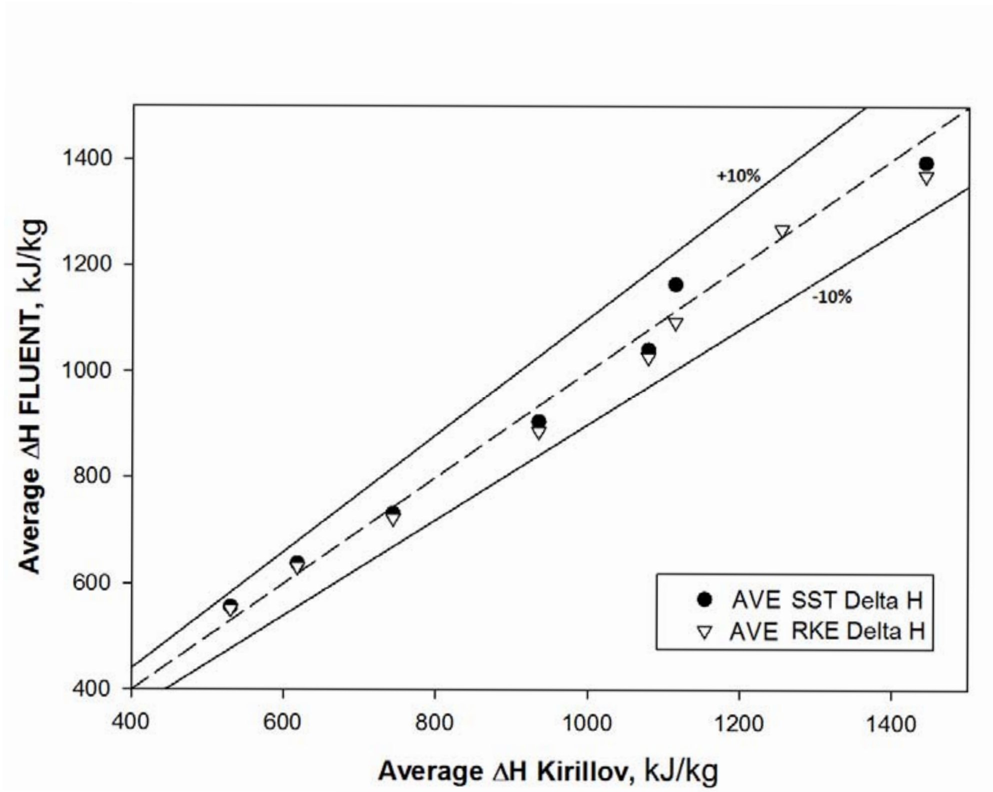

Figure 6: enthalpy balance along the heated length

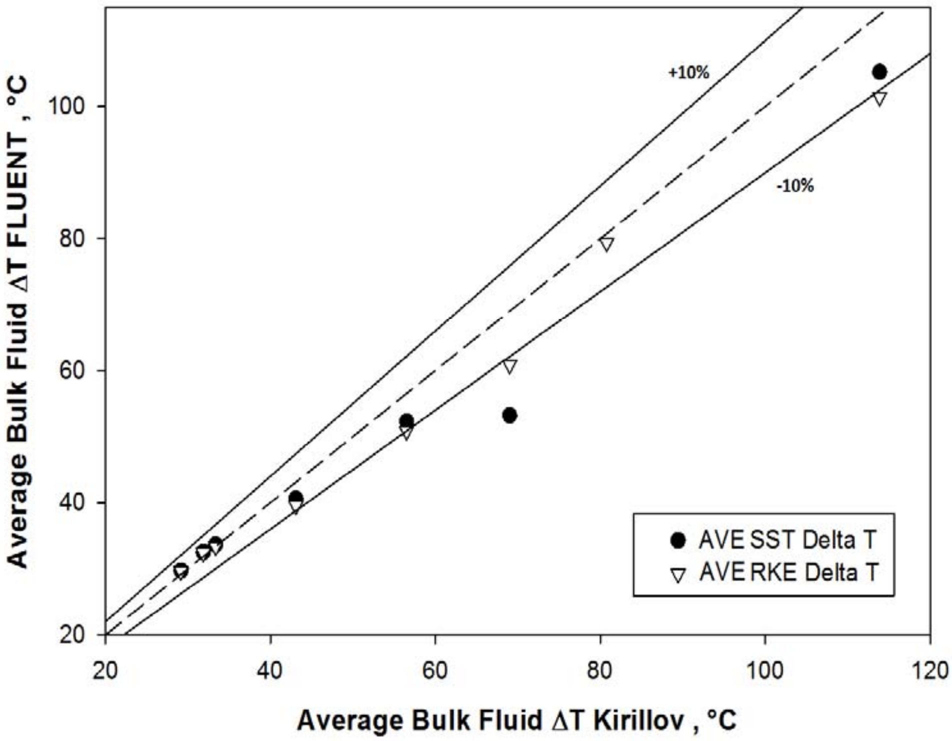

Figure 7: Temperature difference along the heated length

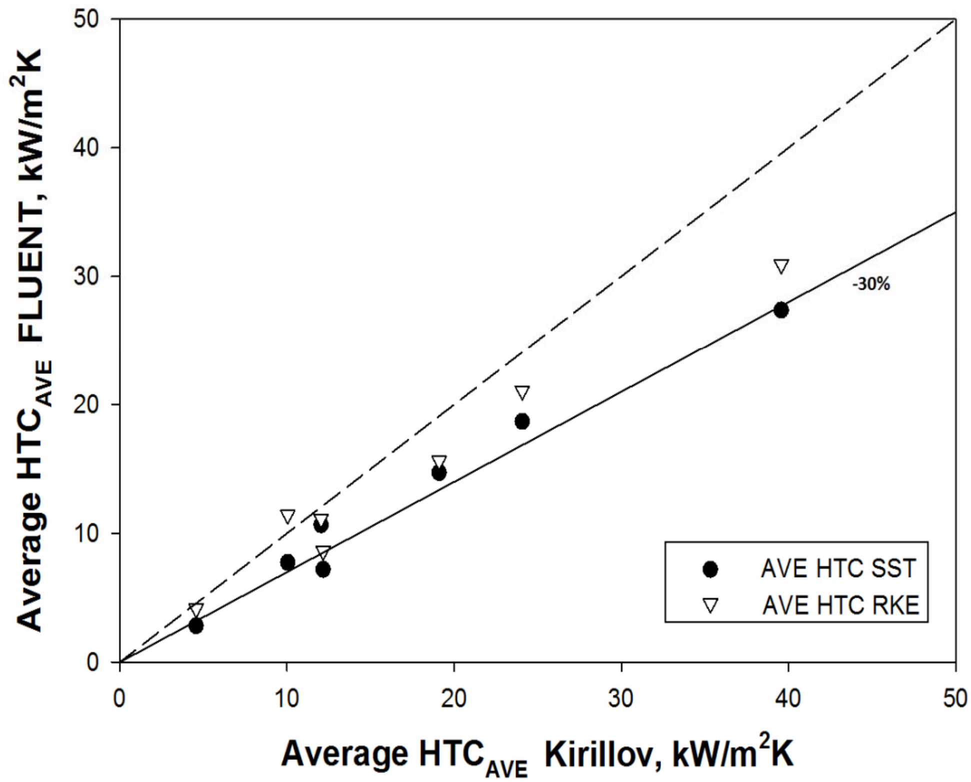

Figure 8: Average heat transfer coefficients

4. Concluding Remarks

A numerical Study of the heat transfer in supercritical water using the CFD code FLUENT-12 was conducted to analyze the 3-D effects occurring in the heat transfer media. The purpose of the study was to assess FLUENT's capability to model the heat transfer problems of supercritical pressure water. The following remarks could be made regarding the overall work:

- The enthalpy balance and temperature rise of the bulk fluid are well resolved.
- The wall temperature is inadequately resolved by the SST k-ω model, while the RKE solutions show no apparent discontinuities in the temperature profile.
- The sub- and supercritical regions can be adequately modeled, but FLUENT-12 has difficulty predicting the pseudocritical transition and the deteriorated heat transfer regimes using the tested models.

Future work will include more in-depth mesh independence studying as additional computational resources become available, testing of the models on the new mesh in each of the heat transfer regimes separately, expanding the dataset to shed a light on the effects of different parameters such as length of the tube, diameter, and pressure effects on the performance of FLUENT-12, and finally moving on to sub-channel modelling of SCWR fuel bundles to observer the code's behaviour when posed with complex 3-D geometries.

5. Acknowledgements

Financial support from the NSERC/NRCan/AECL Generation IV Energy Technologies Program and NSERC Discovery Grants are gratefully acknowledged. The authors would like to express their appreciation to Professor P.L. Kirillov (IPPE, Obninsk, Russia) for providing the dataset with which computations were performed. Dr. Igor Shevchuk and professor Su Jian also deserve acknowledgement for valuable comments and discussions.

6. Nomenclature

H	specific enthalpy, J/kg
k	total turbulent kinetic energy, m^2/s^2
m	mass-flow rate, kg/s
P, p	pressure, MPa
q	heat flux, W/m^2
Q	power or heat-transfer rate, W
R	radius, m
T, t	temperature, °C
Re	Reynolds number

Abbreviations and Acronyms

CANDU	CANada Deuterium Uranium (reactor)
CFD	Computational Fluid Dynamics
DHT	Deteriorated Heat Transfer
EHT	Enhanced Heat Transfer
NHT	Normal Heat Transfer
NIST	National Institute of Standards and Technology
NSERC	Natural Sciences and Engineering Research Council
RKE	Realizable k-ε
SCW	Supercritical pressure Water
SCWR	Supercritical pressure Water Reactor
SST	Shear Stress Transport
UDF	User Defined Function
UOIT	University of Ontario Institute of Technology

Subscripts

ave	average
in	inlet
out	outlet
pc	pseudocritical

Greek letters

ε	dissipation rate of turbulent kinetic energy, m^2/s^3
ω	specific turbulent energy dissipation rate, 1/s
μ	molecular viscosity, μPas
μ_t	eddy viscosity, m^2/s
ρ	density of fluid, kg/m^3
τ_{wall}	shear stress at the wall, Pa

7. References

[1] Gupta, S., Farah, A., King, K., Mokry, S. And Pioro, I. "Developing New Heat-Transfer Correlation for SCW Flow in Vertical Bare Tubes", International Conference on Nuclear Engineering (ICONE-18), 2010, Xi'an.

[2] Dyadyakin, B.V., and Popov, A.S. "Heat Transfer and Thermal Resistance of Tight Seven-rod Bundle, Cooled with Water Flowing at Supercritical Pressures," *Transactions of VTI*, vol. 11, pp. 244-253, 1977.

[3] Sharabi, M. and Ambrosini, W. "Transient 3D Stability Analysis of SCWR Rod Bundle Subchannels by a CFD Code," International Conference on Nuclear Engineering (ICONE-16), 2008, Orlando.

[4] Holloway, M. V. and Beasley, D. E. "Investigation of Swirling Flow in Rod Bundle Subchannels Using CFD," International Conference on Nuclear Engineering (ICONE-16), 2006, Miami.

[5] Muhana, A. and Novog, D. R. "Validation of FLUENT for Prediction of Flow Distribution and Pressure Gradients in a Multi-Branch Header Under Low Flow Conditions," International Conference on Nuclear Engineering (ICONE-16), 2008, Orlando.

[6] Pietralik, J. M. and Smith, B. A. W. "CFD Applicaiton to FAC in Feeder Bends" International Conference on Nuclear Engineering (ICONE-16), 2006, Miami.

[7] Vanyukova, G. V. et al., "Application of CFD-Code to Calculations of Heat Transfer in a Fuel Bundle of SCW Pressure-Channel Reactor," 4th International Symposium on Supercritical Water-Cooled Reactors, 2009, Heidelberg.

[8] Kirillov, P. L. et al., "Experimental Study on Heat Transfer to Supercritical Water Flowing in Vertical Tubes," Proc. of the Int. Conf. GLOBAL-2005 "Nuclear Energy Systems for Future Generation and Global Sustainability, 2005, Tsukuba.

[9] Zahlan, H., Groeneveld, D. C. And Tavoularis, S. "Look-up Table for Trans-Critical Heat Transfer," The 2nd Canada-China Joint Workshop on Supercritical Water Cooled Reactors (CCSC 2010), 2010, Toronto.

[10] Gabarev, B. A., Kuznetsov, Y. N., Pioro, I. L. and Duffey, R. B. , "Experimental Study on Heat Transfer to Supercritical Water Flowing in 6-m Long Vertical Tubes," Conference on Nuclear Engineering (ICONE-15), 2007, Nagoya.

[11] National Institute of Stanards and Technology, "NIST Reference Fluid Thermodynamic and Transport Properties - REFPROP," *NIST Standard Reference Database 23, Ver. 8.0*, vol. Boulder, CO. US Department of Commerce.

[12] Launder, B. E. And Jones, W. P. "The Calculation of Low Reynolds Number Phenomena with a Two-Equation Model of Turbulence," *Int.l J. Heat and Mass Transfer*, vol. 16, no. 6, pp. 1119-1130, 2973.

[13] Wilcox, D. "Simulation of Transition with a Two-Equation Turbulence Model.," *AIAA Journal*, vol. 32, no. 2, pp. 247-255, 1994.

[14] Menter, F. "Two-Equation Eddy-Viscosity Turbulence Models for Engineering Applicaitons," *AIAA Journal*, vol. 32, pp. 1598-1605, 1994.